RESEARCH ARTICLE OPEN ACCESS

Formation and Characterization of Mixed Crystals Based on Bis (Thiourea)Cadmium Chloride and Bis (Thiourea)Cadmium Iodide

I.S. Prameela Kumari[1*] and C.K. Mahadevan
Sree Ayyappa College For women Chunkankadai- 629003, Tamil Nadu ,India.
Physics Research Center, S.T. Hindu College, Nagercoil-629002, Tamil Nadu, India.

Abstract
Bis(thiourea)cadmium chloride(BTCC) and bis(thiourea)cadmium iodide (BTCI) are metal complexes of thiourea having better nonlinear optical properties than KH_2PO_4. An attempt has been made in the present study to form mixed crystals based on BTCC and BTCI (even though their crystal lattices mismatch) from aqueous solutions, the precursors mixed in proper proportions. A total of seven (including the end members) crystals were formed by the free evaporation method and characterized chemically, structurally, thermally, optically and electrically. The X-ray diffraction measurements indicate that $(BTCC)_X(BTCI)_{1-X}$ crystals with x=1.0,0.8 and 0.6 are orthorhombic in structure with space group $Pmn2_1$ and that with x=0.5, 0.4, 0.2 and 0.0 are monoclinic in structure with space group $P2_1/c$. All the grown crystals are found to be thermally stable up to 215 $^{\circ}$C and possessing wide optical transmission window (300-900 nm) which is suitable for NLO applications. The electrical measurements indicate that the grown crystals exhibit a normal dielectric behavior. The results obtained in the present study indicate that mixed crystals can be formed from the isomorphous precursors directly even though the end member's crystals have lattice mismatching.
Key words: Optical materials, Crystal growth, Electrical transport, Optical properties, Nonlinear optics, X-ray diffraction

I. Introduction

The search for new frequency conversion materials over the past two decades concentrated primarily on organic compounds [1]. However, the implementation of organic materials single crystals in practical device applications has been impeded by their often inadequate transparency, poor optical quality and low laser damage threshold. Inorganic materials single crystals have excellent mechanical and thermal properties, but possess relatively modest optical nonlinearities. Hence, recent research is concentrated on semi-organic materials single crystals due to their large nonlinearities, high resistance to laser induced damage, low angular sensitivity and good mechanical hardness [2].

Thiourea molecule is an interesting inorganic matrix modifier due to its large dipole moment, and ability to form extensive network for hydrogen bond [2]. Thiourea, in combination with metal complexes, forms semi-organic compounds having low cut off wavelength and applications for high power frequency conversion. Some of the potential thiourea-metal complexes reported are ; bis(thiourea)cadmium chloride (BTCC) [3-16], bis(thiourea)cadmium iodide(BTCI)[2], bis(thiourea)zinc(II) chloride (BTZC) [17,18], bis(thiourea)cadmium bromide(BTCB)[19] and tetra(thiourea)cadmium tetrathiocyanato zincate (TCTZ) [20].

BTCC has powder second harmonic generation (SHG) effiency as high as 110 times that of quartz. Most of the above crystals have better nonlinear property than that of KH_2PO_4 (KDP).It crystallizes in the orthorhombic system with lattice parameters a=5.812, b=6.485 and c=13.106 Å and lattice volume 494.092(Å)^3[ ].Mg, Co, Ni, Cu, Zn doped crystals have already been grown and characterized [7]. BTCI is a good candidate for electro-optic modulators. It crystallizes in the monoclinic system with lattice parameters a=10.520 Å , b=7.600 Å, c=15.086 Å, and volume 1205.75(Å)^3[2].

Use of multiple components (hybrid materials or alloys) offers a higher degree of flexibility for altering and controlling properties and functionalities of materials. For many emerging technologies, hybrid or alloyed materials with improved physical properties are needed. In order to discover new useful materials, in the present study, we have made an attempt to grow and characterize mixed crystals based on BTCC and BTCI.

A mixed crystal is normally obtained by crystallizing together two or more isomorphous crystals. Isomorphism is not the only condition for the formation of mixed crystal. The conditions for the formation of mixed crystals are: the structures of the two crystals should be of similar type; the bonds in the two crystals should be of similar type; the radii of

the substituent atoms should not differ by more than 15% from that of the smaller one; and the difference between their lattice parameters should be less than 6%.

The precursors used for the growth of BTCC/BTCI crystals are cadmium chloride/cadmium iodide and thiourea. The crystal lattices of BTCC and BTCI do not match and the crystal structures are not isomorphous to each other. So, as per the conditions prescribed for the formation of mixed crystals, it may not be possible for us to form the BTCC-BTCI mixed crystals. Now, the interesting question is how to form the BTCC-BTCI mixed crystals. Considering the method of forming BTCC and BTCI crystals and by making use of the isomorphism of cadmium chloride and cadmium iodide molecules, we attempted to form the BTCC-BTCI mixed crystals and succeeded. Results obtained in our present study are reported and discussed herein.

II. Experimental Procedures

Analytical reagents (AR) grade chemicals were used in the present study. The end members, BTCC/ BTCI crystals, were formed from aqueous solutions of cadmium chloride/ cadmium iodide and thiourea taken in the molecular ratio of 1:2. The expected chemical reactions are:

$$CdCl_2 + 2[CS(NH_2)_2] \longrightarrow Cd[CS(NH_2)_2]_2Cl_2$$
$$CdI_2 + 2[CS(NH_2)_2] \longrightarrow Cd[CS(NH_2)_2]_2I_2$$

Since thiourea has the coordinating capacity to form different phases of metal thiourea complexes, the solutions had to be stirred well to avoid co-precipitation of multiple phases due to any metal impurities present[21]. Tiny single crystals appeared in about 20 days and then grew to significant size, in another about 10 days. Cadmium chloride and cadmium iodide were mixed in the required proportions to form the $(BTCC)_X(BTCI)_{1-X}$ mixed crystals. Similar procedure was followed to form the mixed crystals. The mixed crystals also appeared in about 20 days and grew to significant size in another 10 days. The grown crystals (2 end members + 5 mixed crystals) are found to be stable in atmospheric air and non-hygroscopic. Optically transparent and defect free crystals of considerable size were selected for carrying out the characterization experiments. Single crystal X-ray diffraction (SXRD) were collected at room temperature by using Enraf Nonius CAD-4 single crystal X-ray diffractometer with MoK_α radiation(λ=0.71073Å) to identify the crystal lattice parameters. The SXRD data could not be obtained for the mixed crystals with compositions x=0.4, 0.5 and 0.6, as these crystals were very small to be considered for the measurements. Powder X-ray diffraction (PXRD) data were collected by employing a PANalytical diffractomer with CuK_α radiation (λ=1.54056 Å), scanned over the 2θ range of 10-80 °C at the rate of 1 °/min, to understand the crystallinity of the crystals grown and characterize structurally. The Fourier transform infra-red (FTIR) spectra of all the seven crystals grown were recorded by a BRUKER IFS 66V FTIR spectrometer using the KBr pellet technique in the frequency range 400-4000 cm^{-1} to identify the presence of functional groups. Even though AR grade precursors were used for the formation of single crystals, the data supplied by the manufactures showed the presence of calcium, potassium, sodium and zinc metal impurities up to 0.01 %. In order to understand quantitatively the presence of these metal impurities in the grown crystals, atomic absorption spectroscopic (AAS) analysis was done using an atomic absorption spectrometer (Model name AA-6300). Energy dispersive X-ray spectroscopic (EDX) analysis was carried out, to quantitatively estimate, the presence of chlorine and iodine atoms in the mixed crystals by using a JOEL/EO JSM-6390 scanning electron microscope. In order to understand the thermal behavior of the grown crystals, thermogravimetric analysis (TGA) and differential thermal analysis (DTA) were carried out simultaneously by employing a Perkin Elmer thermal analyzer (Model: PYRIS DIAMOND) in nitrogen atmosphere heated from 30-800 °C. The UV-Vis-NIR absorption spectra were recorded using SHIMADZU UV 1700 spectrometer with a medium scan interval 0.2 in the wavelength range 200-900 nm. The second harmonic generation (SHG) test was carried out on all the grown crystals using the Kurtz and Perry powder technique [22]. The micro crystalline powdered sample was packed in a capillary tube of diameter 0.154 mm. The powder sample, with an average size of 100-150 µm, was illuminated with a Q switched mode-locked Nd^+:YAG laser of pulse width 8ns at wavelength of 1064nm fundamental radiation. For the SHG measurement micro crystalline material of KDP was used for comparison. Only 4 single crystals (with compositions x=1.0, 0.8, 0.2 and 0.0) were significantly large in size. So, these crystals with high transparency and large surface defect-free size greater than 3 mm were selected and used for the electrical (both DC and AC) measurements. Opposite faces of the selected crystals were polished and coated with good quality graphite to obtain a conductive surface layer. The dimensions of the crystals were measured using a traveling microscope (LC=0.001 cm). In order to characterize electrically all the crystals grown, the crystal samples were powdered and compacted into disc-shaped pellets of 13 mm diameter by 5 tone hydraulic pressure. Pellets of crystal samples with composition x=1.0, 0.8, 0.2 and 0.0 were also considered for comparison purpose. The flat surfaces of the pellets were coated with good quality graphite to obtain a good

conductive layer. Also the dimensions of the pellets were measured using a traveling microscope. The electrical measurements (both DC and AC) were carried out for 4 crystal samples and 7 crystalline pellets using the conventional two -probe technique (parallel plate capacitor method)[23-25] at various temperatures ranging from 35-100 °C for samples with x=1.0,0.5 and0.0 and 0.0 and 35-70 °C for others. .The temperature range was fixed by considering the thermal stability of the grown crystals understood from their TGA patterns. The AC electrical measurements were carried out with 5 different frequencies, viz. 100 Hz, 1 KHz,10 kHz, 100 kHz and 1 MHz .The sample was initially heated up to the maximum temperature considered and kept for about 1 hour to thermally homogenize it. The observations were made while cooling the sample. The DC electrical conductivity (σ_{dc}) was calculated using the relation:

$\sigma_{dc} = d / (RA)$----------(1)

Where R is the measured resistance, d is the thickness of the sample, and A is the area of the face in contact with the electrode. The resistance was measured using a million meg-ohm meter. The temperature was controlled to an accuracy of ± 1 °C. The capacitance and dielectric loss factor (tanδ) were measured by using an LCR meter (Agilent 4284-A) .The dielectric constant(ε_r) of the crystalline pellet was calculated using the relation:

$\varepsilon_r = C_{pellet} / C_{air}$ ----------(2)

where C_{pellet} is the measured capacitance of the pellet and C_{air} is the air capacitance for the same thickness with the pellet. The dielectric constant (ε_r) of the crystal sample (as the area of crystal touching the electrode was smaller than the electrode area of the parallel plate capacitor) was calculated using Mahadevans formula[26,27]:

$\varepsilon_r = (A_{air}/A_{crys}) \{[C_{crys}-C_{air}(1-A_{crys}/A_{air})] / C_{air}\}$ -----(3)

where A_{crys} is the area of the crystal touching the electrode, A_{air} is the area of electrode, C_{crys} is the capacitance of the crystal and C_{air} is the capacitance for the same thickness with crystal. The AC electrical conductivity (σ_{dc}) was calculated using the relation:

$\sigma_{ac} = \varepsilon_0 \varepsilon_r \omega \tan\delta$----------(4)

where ε_0 is the permittivity of free space and ω is the angular frequency of the applied field.

III. Results and discussion

3.1 Crystals growth

Photographs of the sample crystals grown in the present study are shown in Figure 1. All the seven crystals grown are stable in atmospheric air, non-hygroscopic and transparent. Size of the crystals with middle compositions x=0.6, 0.5 and 0.4 are small. Moreover the mixed crystals are less transparent when compared to the end member crystals. The estimated (through AAS data) concentrations of natural impurities present in the crystals are compared in Table. 1 with the concentrations of those available in the precursors used for the growth of single crystals.

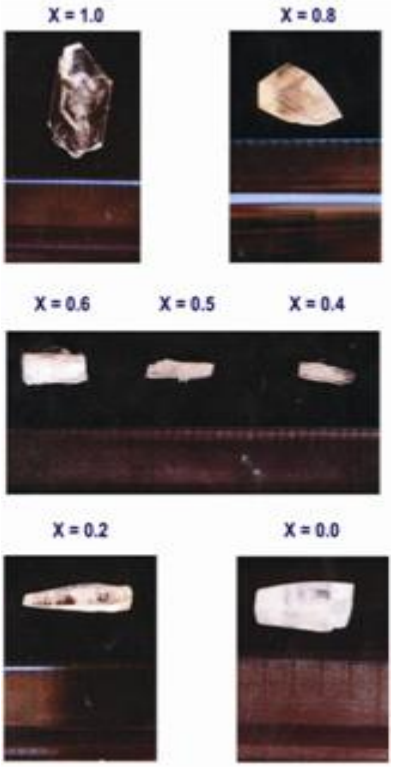

Figure 1: Photograph of as grown $(BTCC)_x$ $(BTCI)_{1-x}$ mixed crystals (x = 1.0, 0.8, 0.6, 0.5, 0.4, 0.2 & 0.0)

Table 1 : Estimated concentrations of natural impurities present in the crystals and concentrations of those available in the precursors used for crystal growth of single crystals

$(BTCC)_x(BTCI)_{1-x}$ with	Calcium	Potassium	Sodium	Zinc

	Limits of impurities		**Limits of impurities**		**Limits of impurities**		**Limits of impurities**	
	%	**ppm**	**%**	**ppm**	**%**	**ppm**	**%**	**ppm**
x =1.0 (BTCC)	0.01	193.67	0.01	72.913	0.01	252.14	0.01	26.701
x = 0.8	0.01	337.38	0.02	104.60	0.02	176.39	0.01	33.709
x = 0.6	0.01	260.72	0.02	105.70	0.02	175.85	0.01	18.24
x = 0.5	0.01	257.10	0.02	141.46	0.02	214.48	0.01	158.35
x = 0.4	0.01	333.18	0.02	119.46	0.02	147.28	0.01	226.65
x = 0.2	0.01	506.74	0.02	152.12	0.02	238.48	0.01	41.1917
x = 0.0 (BTCI)	-	-	0.01	113.964	0.01	160.06	-	-

3.2. Lattice variations and chemical compositions

The observed lattice parameters, space group and crystal system through SXRD analysis are given in Table 2. It can be seen that the crystals with compositions x=1.0 and 0.8 belong to orthorhombic crystal system and those with compositions x=0.2 and 0.0 belong to monoclinic crystal system. The lattice parameters observed for the end members (BTCC and BTCI) compare well with those reported in the literature [5, 2].

Table 2: The lattice parameters, space groups and crystal systems observed through SXRD analysis for the grown $(BTCC)_x (BTCI)_{1-x}$ crystals

Mixed crystal with x values	**Lattice parameters**				**Volume $(Å)^3$**	**Space group**	**Crystal system**
	a(Å)	**b(Å)**	**c(Å)**	**β^0**			
BTCC (x = 1.0)	5.815	6.461	13.116	90	493.0	$Pmn2_1$	Orthorhombic
x = 0.8	5.818	6.481	13.120	90	494.8	$Pmn2_1$	Orthorhombic
x = 0.2	10.475	7.625	15.094	91.16	1205.3	$P2_1/c$	Monoclinic
BTCI (x = 0.0)	10.479	7.642	15.138	91.04	1202.0	$P2_1/c$	Monoclinic

The indexed PXRD patterns recorded are shown in Figure 2. Appearance of strong and sharp peaks confirms the crystalline nature of the crystals grown.

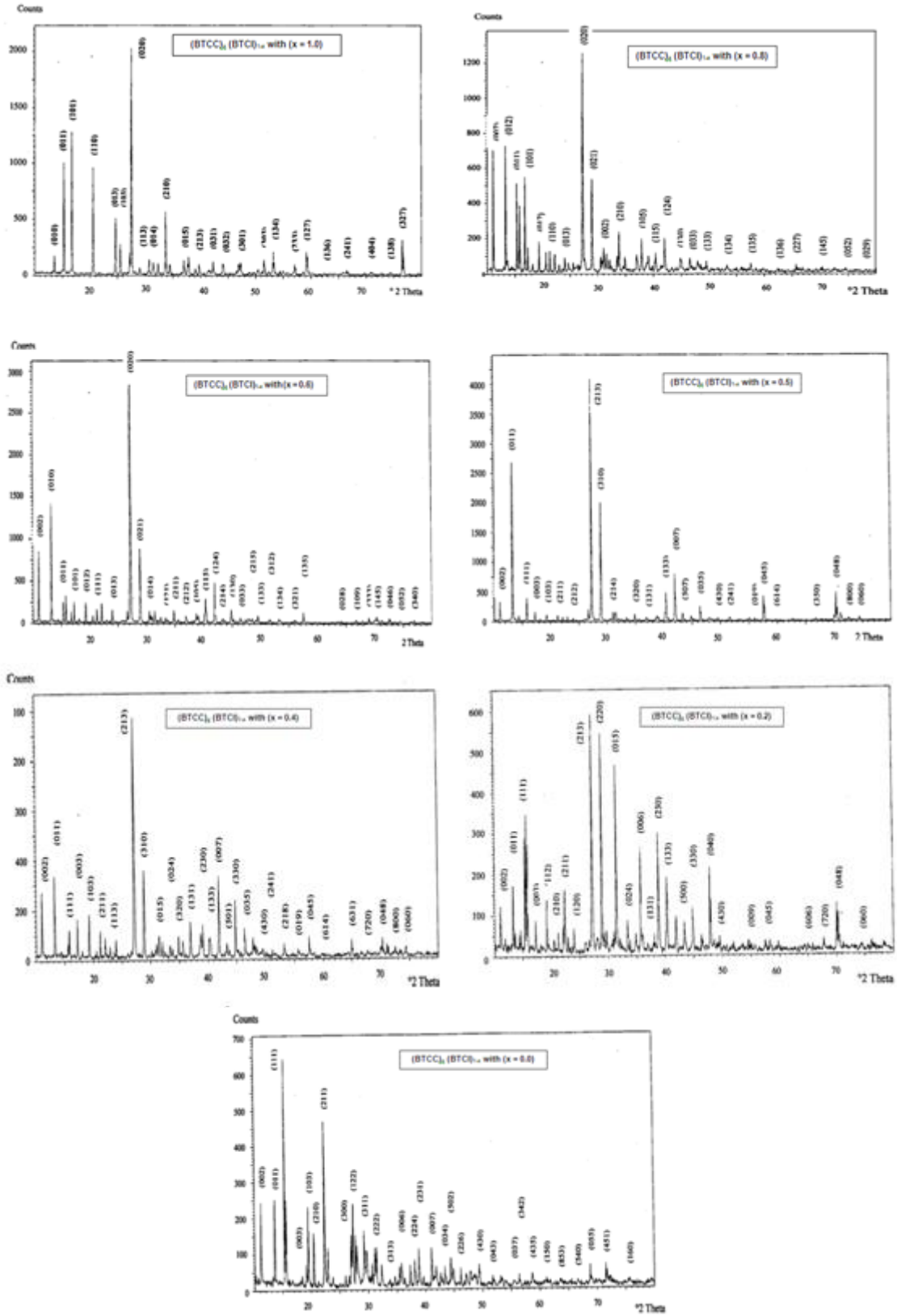

Figure 2: PXRD patterns for the grown $(BTCC)_x(BTCI)_{1-x}$ mixed crystals, (x = 1.0, 0.8, 0.6, 0.5, 0.4, 0.2 & 0.0)

The observed FTIR spectra are shown in Figure 3. The FTIR bands of end members observed in the present study are compared in Table 3 with those of thiourea and end members available in the literature. The vibrational band assignments for the mixed crystals grown in the present study are given in Table 4.

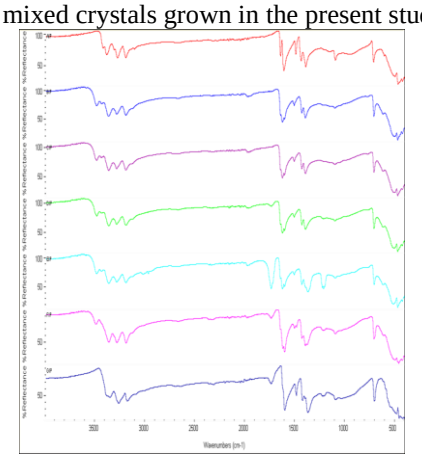

Figure 3 : The FTIR spectra for the grown $(BTCC)_x(BTCI)_{1-x}$ mixed crystals (x = 1.0, 0.8, 0.6, 0.5, 0.4, 0.2 & 0.0 from top to bottom)

Table 7: Comparison of FTIR bands of end members (BTCC (x = 1.0) and BTCI (x = 0.0)) observed in the present study with those of Thiourea

Wave numbers(cm^{-1}) for					
Thiourea	**BTCC (Literature [196])**	**BTCC (Experiment)**	**BTCI (Literature [5])**	**BTCI (Experiment)**	**Band assignment**
411	411	-	-	-	δ_s(N-C-N)
469	478	-	-	-	δ_s(S-C-N)
494	551	502.2	516.0	484.3	δ_{as}(N-C-N)
740	716	714.2	712	707.4	γ_s(C=S)
910	-	956.5	-	-	γ_s(N-C-N)
1089	- 1102	1098.5 1156.8	1095 -	1095.5 1215.8	γ_s(N-C-N)
1417	1399	1394.7	1390	1372.8	γ_{as}(C=S)
1470	1442 1496	1440.6 1494.5	- 1490	1428.0 1489.3	γ_{as}(C-N) γ_{as}(N-C-N)
1627	1622 1649 2941	1613.5 1646.9 -	1610 - -	1604.8 1739.8 2698.3	$\delta_{as}(NH_2)$
- 3167	- 3202	3109.8 3195.6	- 3192	- 3181.6	$\gamma_s(NH_2)$
3280	3287	3278.8	-	3266.5	$\gamma_s(NH_2)$
3776	3372 3431	3387.5 3423.1	3304 -	3356.2 -	$\gamma_{as}(NH_2)$

δ_s – Symmetric bending, δ_{as} – asymmetric bending
γ_s – Symmetric stretching, γ_{as} – asymmetric stretching

Table 4: The vibrational band assignments for the grown crystals($(BTCC)_x$ $(BTCI)_{1-x}$ [with x = 0.8, 0.6, 0.5, 0.4 and 0.2 0.0])

X = 0.8	X = 0.6	X = 0.5	X = 0.4	X = 0.2	Band assignment
507.4 620.6	507.8 621.6	514.5 622.0	515.4 621.5	504.7	δ_{as}(N-C-N)
711.9	711.8	711.4	710.7	711.6	γ_s(C=S)
1100.9	1100.9	1100.7 1215.8	1096.2 1215.8 1229.0	1098.8 1215.6	γ_s(C-N) γ_s(N-C-N)
1398.8	1398.9	1398.6	1369.1	1380.2 1399.8	γ_{as}(C=S)
1433.9 1511.4	1433.6 1511.3	1433.2 1511.4	1433.3 1511.4	1433.1 1507.5	γ_{as}(C-N) γ_{as}(N-C-N)
1607.2 1628.5	1606.8 1628	1606.4 1627.0 1739.3	1605.8 1628.9 1739.5	1605.5 1623.7 1739.3	$\delta_{as}(NH_2)$
3195.1	3195.5	3194.3	2970.1 3027.1 3194.7	2677.7 3193.5	$\gamma_s(NH_2)$
3288.4	3288.8	3287.6	3288.3	3285.0	$\gamma_s(NH_2)$
3367.7 3436.7 3486.8	3367.1 3440.3 3488.2	3367.2 3438.6 3487.3	3367.3 3440.5 3486.7	3367.7 3493.7 -	$\gamma_{as}(NH_2)$

δ_s – symmetric bending, δ_{as} – asymmetric bending
γ_s – symmetric stretching, γ_{as} – asymmetric stretching

The FTIR spectra observed for the mixed crystals show a shift in the frequency bands in the low frequency region. This conforms the metal coordination with thiourea [28].The broad envelope observed within 2690 and 3430 cm^{-1} corresponds to the symmetric and asymmetric stretching modes of NH_2 grouping of cadmium coordinated thiourea. The other bands of thiourea are not shifted to lower frequencies on the formation of cadmium thiourea complex.

This indicates that nitrogen to cadmium bonds are absent in the coordination compounds. The absorption bands observed at 1470 and 1089 cm^{-1} for thiourea have been assigned to the N-C-N stretching vibration [29]. For the crystals grown in the present study, frequencies corresponding to the above vibration are found to be increased. This result can be attributed to the increase the double bond character of carbon to nitrogen bond on complex formation. The C=S stretching of thiourea (1417 cm^{-1}) is found to be shifted to lower values in the spectra observed for the grown crystals. This clearly indicates the coordination of sulfur with cadmium (metal)[30]. On coordination through sulfur, the nature of vibration is slightly changed. C=N stretching vibration(1089cm^{-1}) of thiourea is found to be shifted to higher values in the spectra observed for the mixed crystals. This clearly establishes the delocalization of nitrogen lone pair electrons over carbon-sulfur bond. This is essential for the NLO property of any material. The vibration (740 cm^{-1}) of thiourea is found to be shifted to lower values in the spectra observed for the grown crystals. This lowering of frequency can be attributed to the decrease in double bond character of carbon to sulfur bond on complex formation. Absence of shifting to lower frequency, narrowing and broadening of high frequency absorption bands observed clearly indicates the incorporation of more number of chlorine and iodine ions.

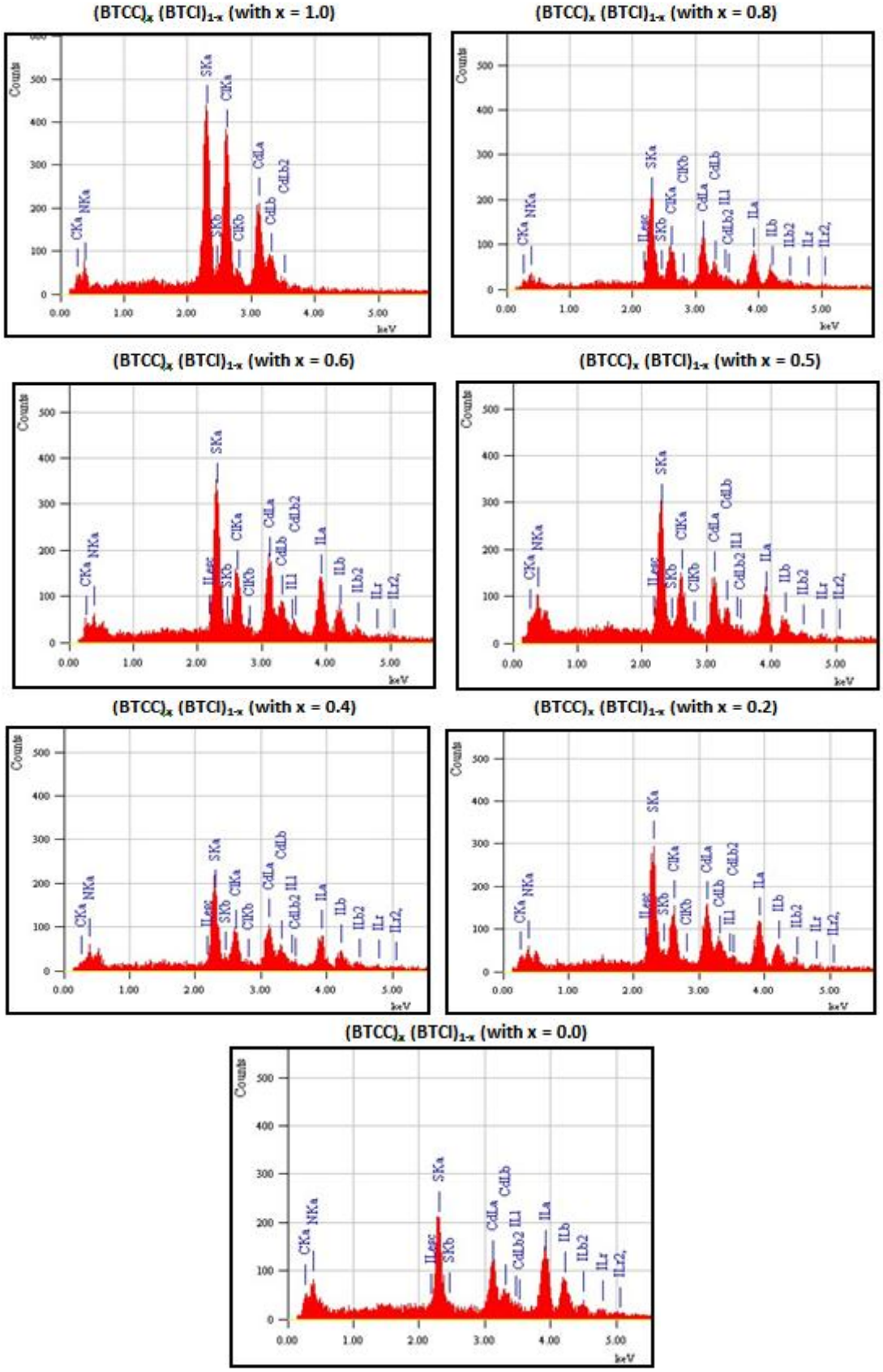

Figure 4: EDX spectra observed for the $(BTCC)_x(BTCI)_{1-x}$ crystals (x = 1.0, 0.8, 0.6, 0.5, 0.4, 0.2 and 0.0)

The EDX spectra observed in the present study are shown in Figure 4. The observed spectra indicate clearly the formation of mixed crystals. Thus the present study indicates that BTCC-BTCI mixed crystals can be formed from the precursors even though the crystal lattices of BTCC and BTCI mismatch.

3.3 Optical and thermal properties

The UV-Vis –NIR absorption spectra observed in the present study are shown in Figure 5. All the grown crystals exhibit wide transmission window in the visible and NIR regions. This enables them to be potential candidates for opto-electronic application. The lower cut off wavelengths lies within 330 nm (see Table 6). Efficient nonlinear optical crystals have an optical transparency lower cut off wavelengths between 200 and 400 nm [31]. The low absorption in the visible and NIR regions along with low cut off wavelengths confirm the suitability of the grown crystals for NLOapplications.

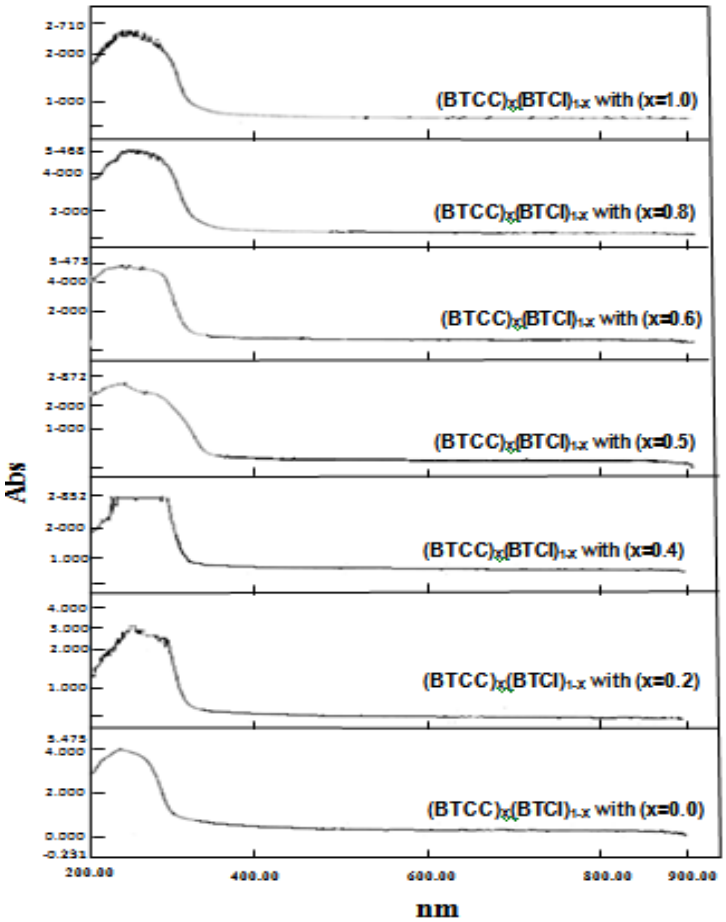

Figure 5: UV-Vis-NIR spectra observed for the $(BTCC)_x(BTCI)_{1-x}$ crystals (x = 1.0, 0.8, 0.6, 0.5, 0.4, 0.2 and 0.0)

The SHG efficiencies observed for all the grown crystals are given in Table 6 .SHG efficiencies of BTCC observed in the present study (7 times that of KDP) compares well that reported in the literature (6.6 times that of KDP) [8].For the mixed crystals grown, it seen that the SHG efficiency decreases with the decrease of x from 1.0 to 0.5 and then increases with that from 0.5 to0.0. This indicates that forming mixed crystals with BTCC and BTCI leads to reduction in SHG efficiency.

Table 5: The cut off wavelength, SHG efficiencies and melting points observed for the grown crystals

$(BTCC)_x(BTCI)_{1-x}$ crystal with	Cut off wavelength (nm)	SHG efficiencies (in KDP unit)	Melting point (°C)
x = 1.0 (BTCC)	300	7 times KDP	215
x = 0.8	307	1.11 times KDP	74

x = 0.6	307	0.16 times KDP	79
x = 0.5	330	0.13 times KDP	143
x =0..4	296	0.24 times KDP	80
x = 0.2	317	0.55 times KDP	80
x = 0.0 (BTCI)	317	0.94 times KDP	140

The TGA and DTA patterns obtained in the present study for all the seven crystals grown are shown in Figure 6. Melting points were also estimated from these patterns which are given in Table 6. The TGA and DTA curves observed for the end members (BTCC and BTCI) compare well those observed by the earlier authors [5, 2]

Figure 6: TGA and DTA curves observed for the $(BTCC)_x(BTCI)_{1-x}$ crystals (x = 1.0, 0.8, 0.6, 0.5, 0.4, 0.2 & 0.0)

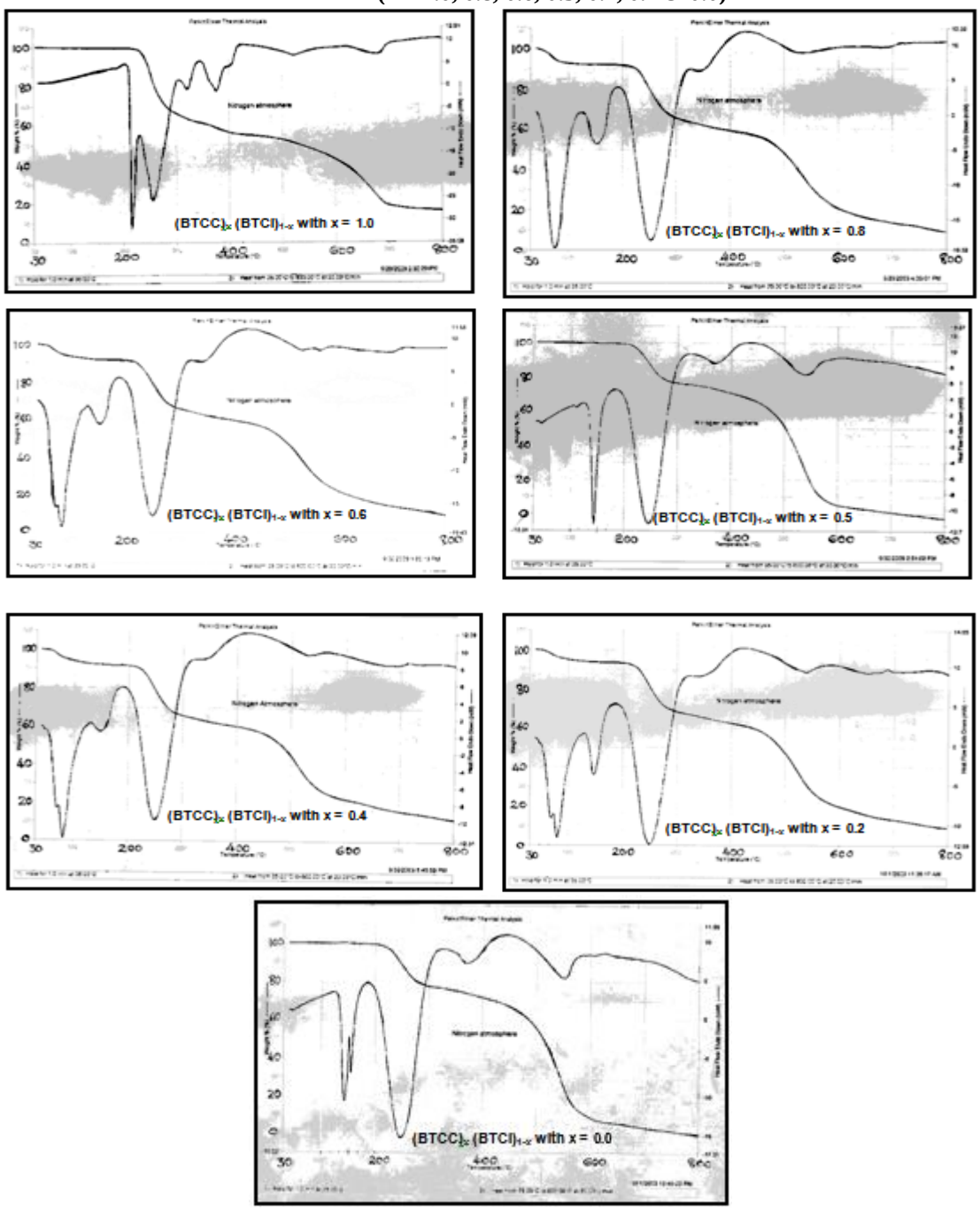

A small weight loss observed in the case of mixed crystals with x=0.2, 0.4, 0.6 and 0.8 beyond 60 °C may be due to absorption of water. Generally all the seven grown crystals exhibit no decomposition at least up to 215 °C. The weight loss observed beyond this temperature may be due to the decomposition of the material. The TGA curves show three stages of weight loss patterns when the materials were heated from 30 °C to 800 °C. The major weight loss occurs in low temperature region which begins around 200 °C and ends around 600 °C with removal of gases like chloride, iodine, etc. The residue that remains after all the decomposition process is only around 10 % which may be carbon mass.

The DTA patterns show sharp endothermic peaks below 200 °C which may be due to the melting of the compound. The other minor endotherms occurring at high temperatures may be due to different stages of decomposition of the substance. The end members (x=0.0 and 1.0) and the mixed crystal with x=0.5 have higher melting points(215°C 140 °C and143°C) respectively whereas the other mixed crystals with x=0.8 ,0.6 ,0.4 and 0.2 have lower melting points (7 °C,79 °C,80 °C and80 °C) respectively. This indicates that the mixed crystals (except that with x=0.5) exhibit less thermal stability.

3.4 Electrical properties

The DC conductivities observed in the present study are shown in Figure 7 and 8. The σ_{dc} values in the temperature region studied are found to increase with the Increase in temperature for all the four bulk crystals and seven crystalline pellets .In the case of bulk crystals, σ_{dc} decreases with the increase in x values (composition) in a systematic way. This indicates that the, σ_{dc} is more for BTCC. All the crystalline pellets exhibit less conductivity when compared to the bulk crystals. This can be attributed to the porosity of the crystalline pellets. Moreover, the conductivity varies nonlinearly with composition at all temperatures for the crystalline pellets.

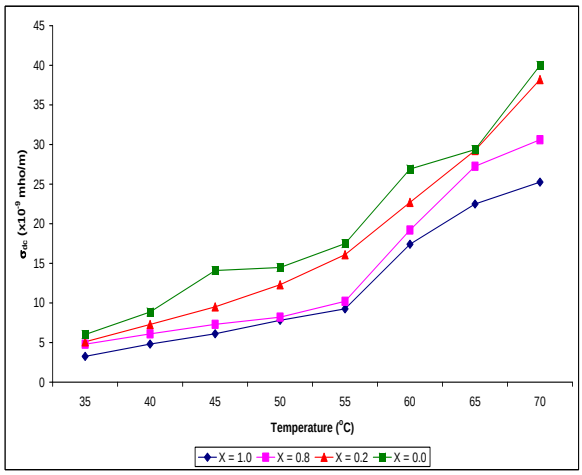

Figure 7: DC conductivity observed for the $(BTCC)_x$ $(BTCI)_{1-x}$ mixed crystals (x = 1.0, 0.8, 0.2, 0.0)

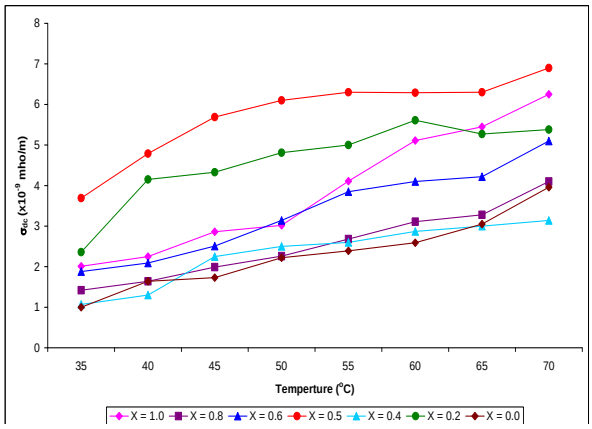

Figure 8: DC conductivity observed for the $(BTCC)_x$ $(BTCI)_{1-x}$ crystalline pellets (x = 1.0, 0.8, 0.6, 0.5, 0.4, 0.2 & 0.0)

Electrical conductivity depends on the thermal treatment of crystals even in pure one. Another dependence is related to degree of solubility of impurities introduced into the crystal. The concentration of impurities dissolved in the lattice increases. If for a certain temperature, the concentration of impurities is higher than allowable due to solubility limit, then the excess substance precipitates to form a new phase-the precipitate. The precipitate tends to form a dislocation which may be revealed by electron microscopy; the crystal may take on a milky aspect. This effect influences the electrical conductivity [32]. In the present study, presence of natural impurities in the grown crystals (see Table 1) is expected to affect the electrical conductivity significantly. Thus, the observed nonlinear variation of electrical conduction with composition can be explained due to the enhanced diffusion of charge carriers along dislocation and grain boundaries.

The dielectric parameters, viz. dielectric constants(ε_r), dielectric loss factor (tanδ) and AC electrical conductivities (σ_{ac}) observed in the present study are shown in Figure 9-11. The composition dependences of these three parameters at the frequency of 1 kHz are shown in Figure 12-14. The ε_r and tanδ values are found to increase with the increase in temperature and decrease with the increase in frequency. The σ_{ac} value is found to increase with the increase in both temperature and frequency. Moreover, the σ_{ac} values are found to be significantly more than the σ_{dc} values. This is considered to be a normal dielectric behavior.

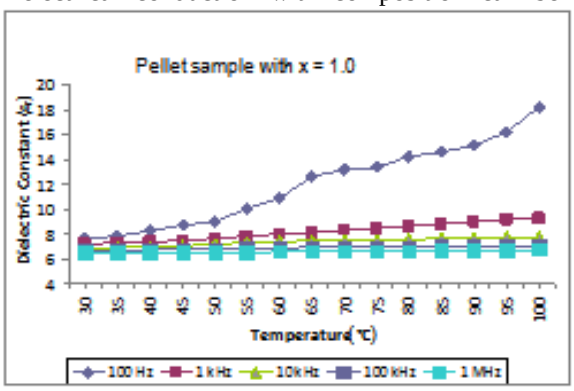

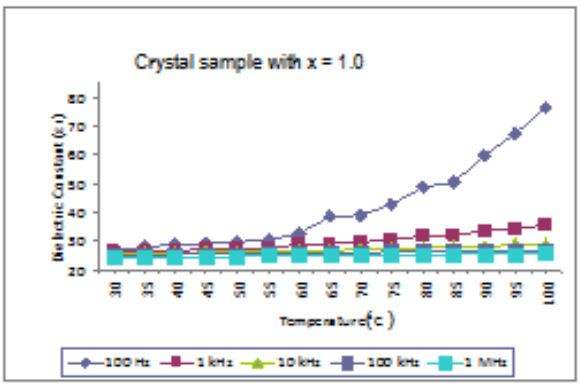

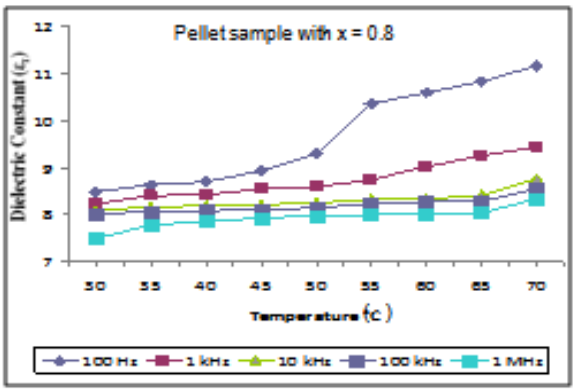

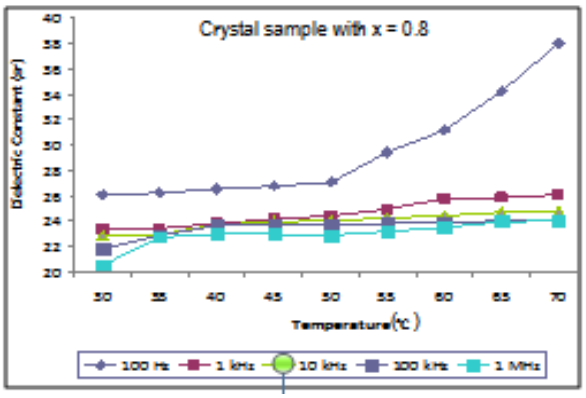

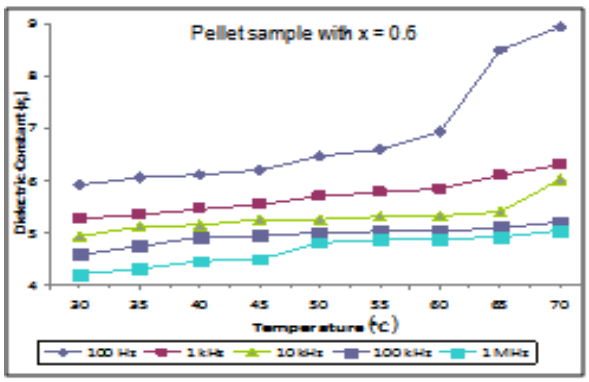

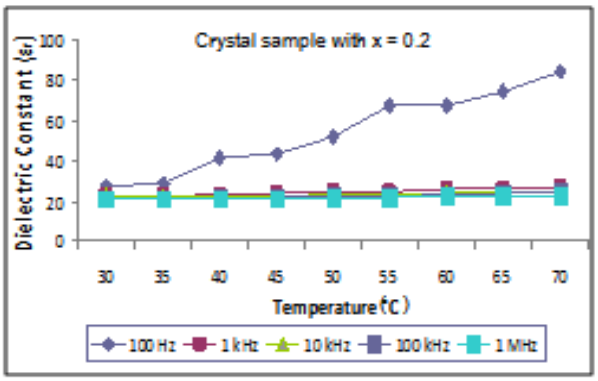

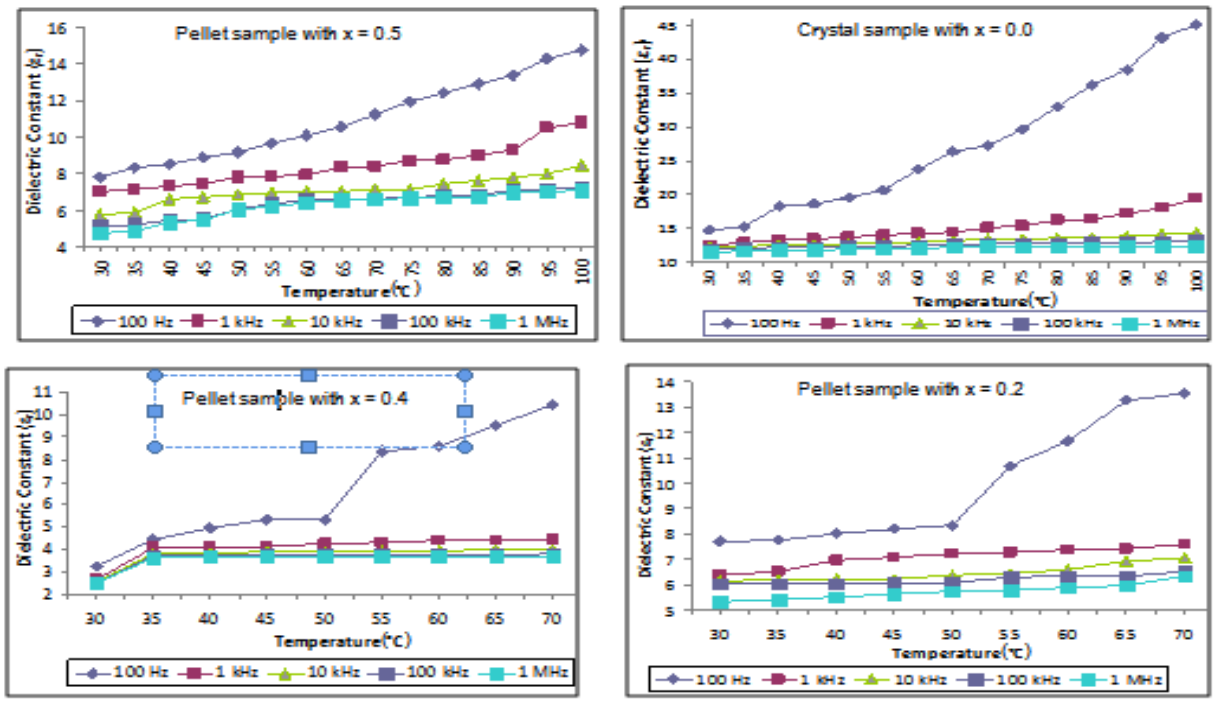

Figure 9: Dielectric constants observed for the $(BTCC)_x$ $(BTCI)_{1-x}$ crystals (x = 1.0, 0.8, 0.2, 0.0) and crystalline pellets (x = 1.0, 0.8, 0.6, 0.5, 0.4, 0.2 & 0.0)

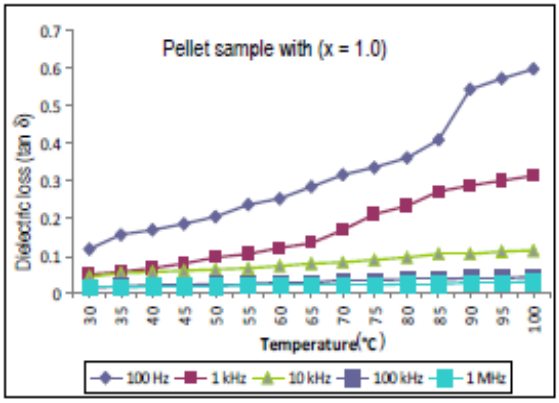
Pellet sample with (x = 1.0)
Dielectric loss (tan δ)
Temperature(°C)
100 Hz
1 kHz
10 kHz
100 kHz
1 MHz

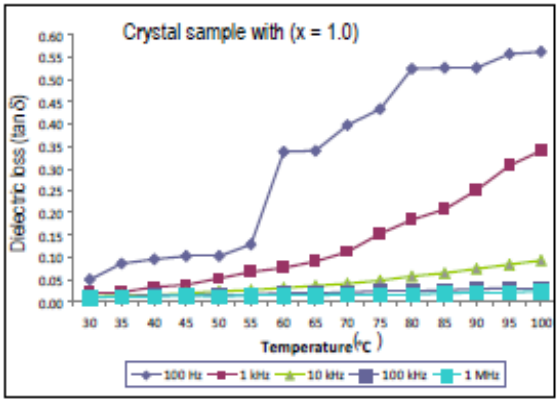
Crystal sample with (x = 1.0)
Dielectric loss (tan δ)
Temperature(°C)
100 Hz
1 kHz
10 kHz
100 kHz
1 MHz

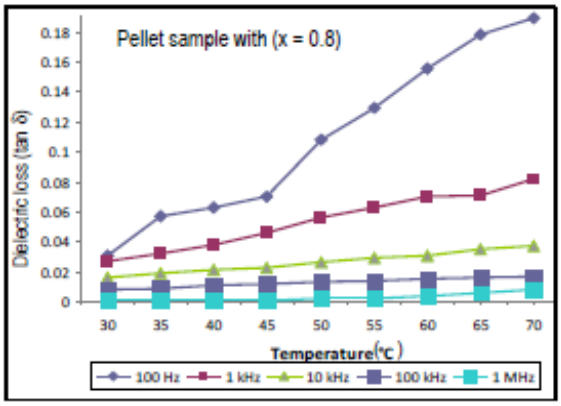
Pellet sample with (x = 0.8)
Dielectric loss (tan δ)
Temperature(°C)
100 Hz
1 kHz
10 kHz
100 kHz
1 MHz

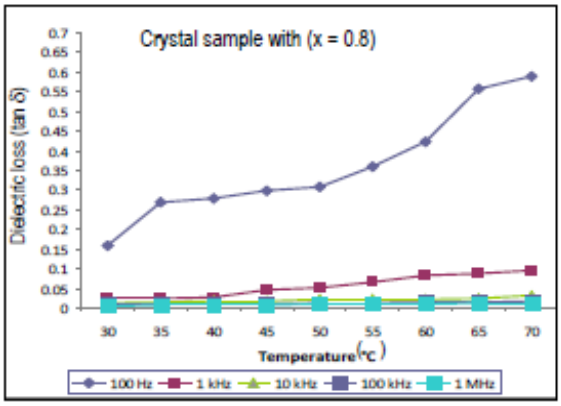
Crystal sample with (x = 0.8)
Dielectric loss (tan δ)
Temperature(°C)
100 Hz
1 kHz
10 kHz
100 kHz
1 MHz

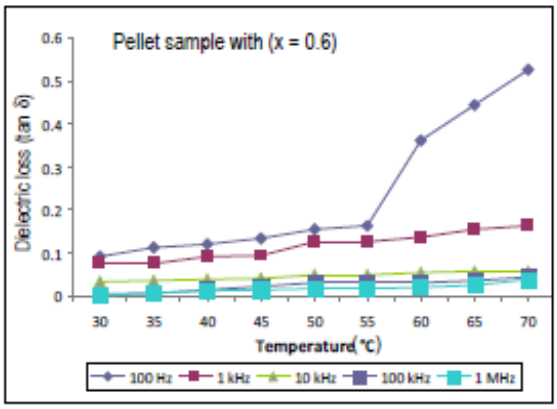
Pellet sample with (x = 0.6)
Dielectric loss (tan δ)
Temperature(°C)
100 Hz
1 kHz
10 kHz
100 kHz
1 MHz

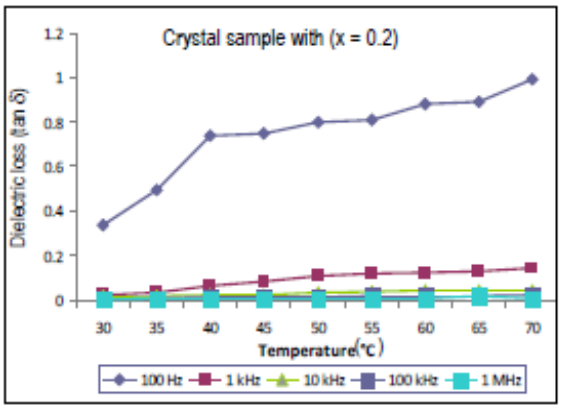
Crystal sample with (x = 0.2)
Dielectric loss (tan δ)
Temperature(°C)
100 Hz
1 kHz
10 kHz
100 kHz
1 MHz

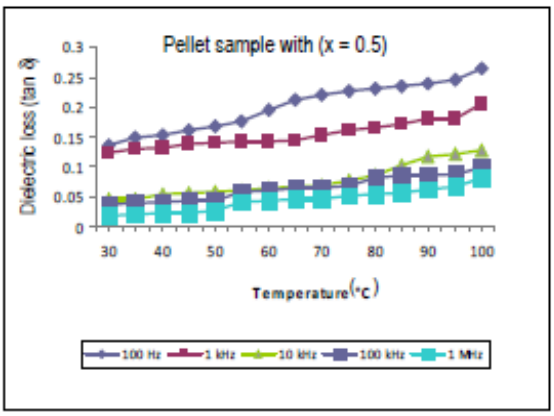
Pellet sample with (x = 0.5)
Dielectric loss (tan δ)
Temperature(°C)
100 Hz
1 kHz
10 kHz
100 kHz
1 MHz

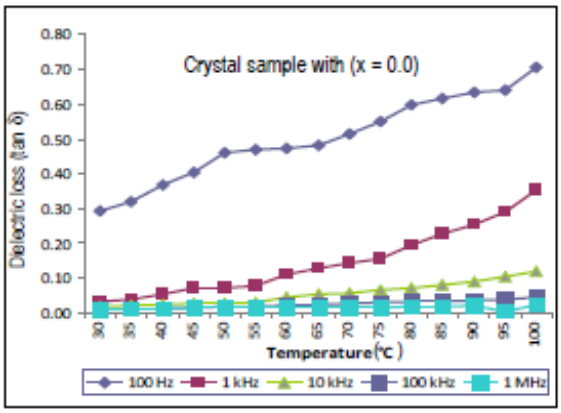
Crystal sample with (x = 0.0)
Dielectric loss (tan δ)
Temperature(°C)
100 Hz
1 kHz
10 kHz
100 kHz
1 MHz

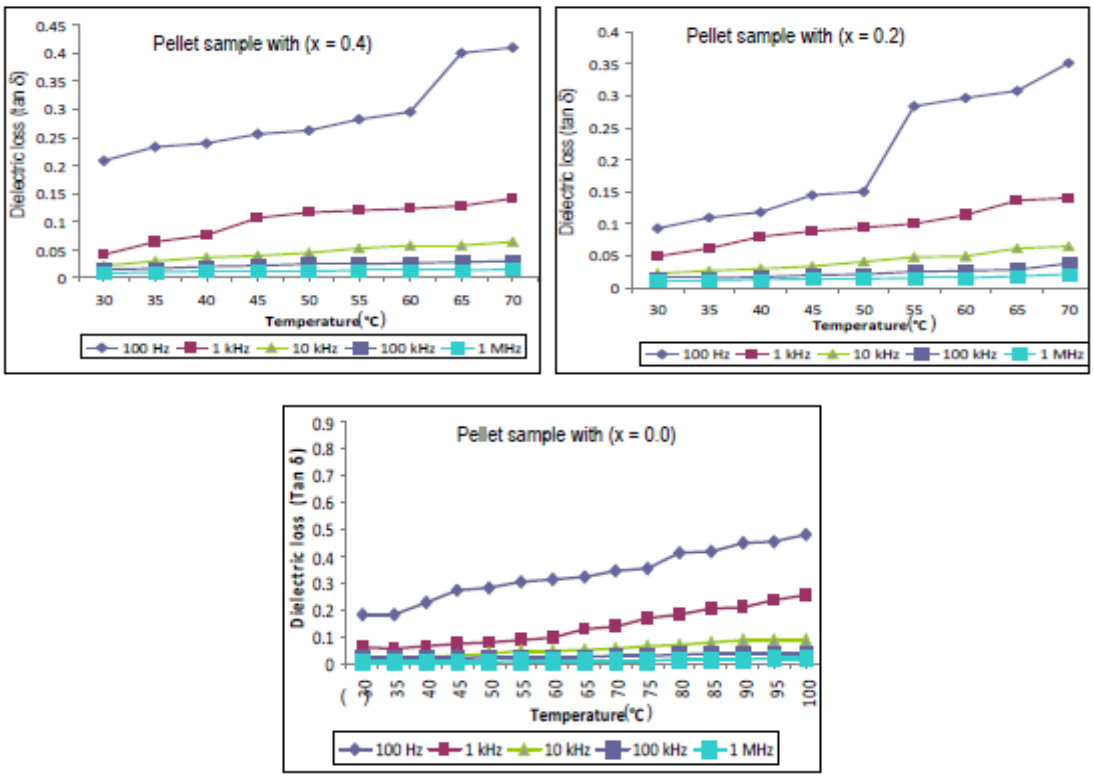

Figure 10: Dielectric loss factors **observed for $(BTCC)_x$ $(BTCI)_{1-x}$ crystals (x = 1.0, 0.8, 0.2, 0.0) and crystalline pellets (x = 1.0, 0.8, 0.6, 0.5, 0.4, 0.2 & 0.0)**

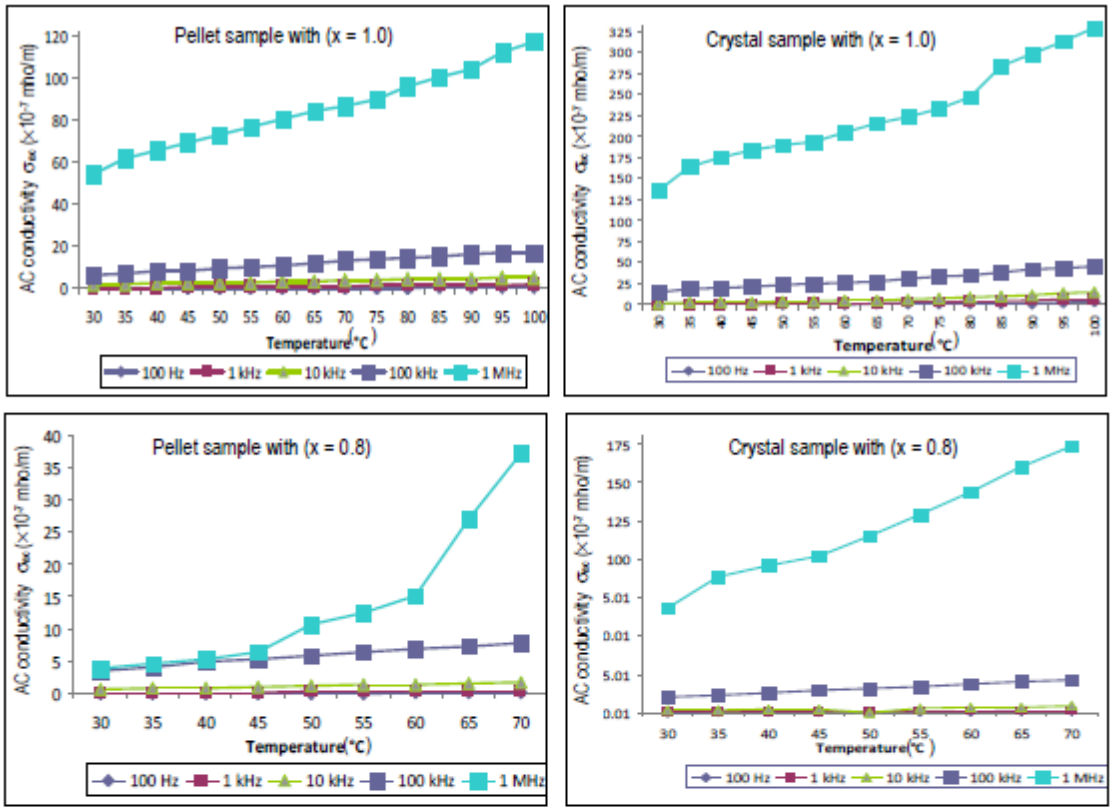

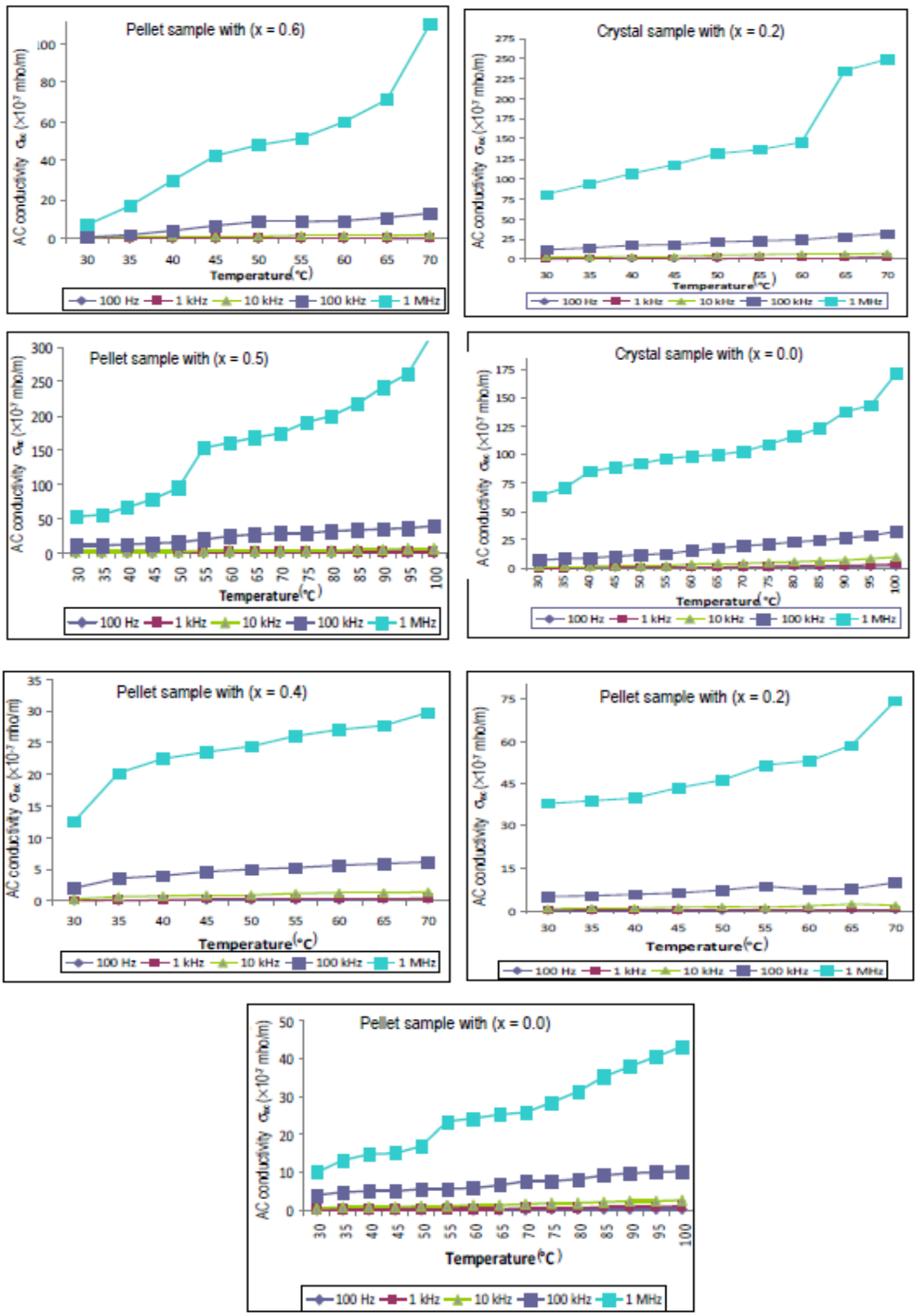

Figure 11: AC electrical conductivities observed for $(BTCC)_x$ $(BTCI)_{1-x}$ crystals (x = 1.0, 0.8, 0.2, 0.0) and crystalline pellets (x = 1.0, 0.8, 0.6, 0.5, 0.4, 0.2 & 0.0)

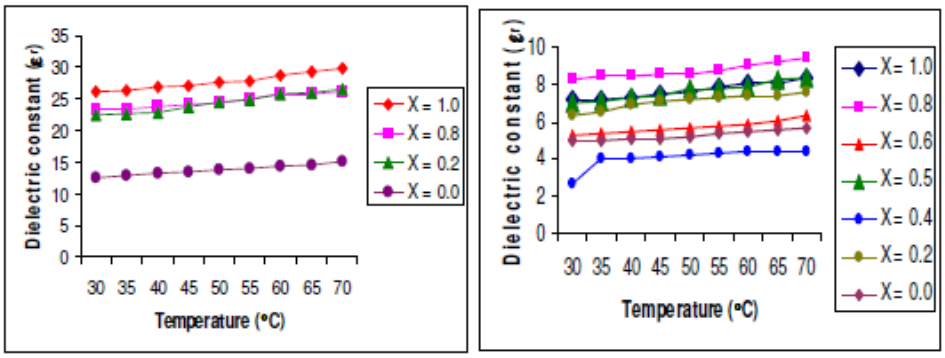

Figure 12: Composition dependence of dielectric constants for the crystals and crystalline pellets

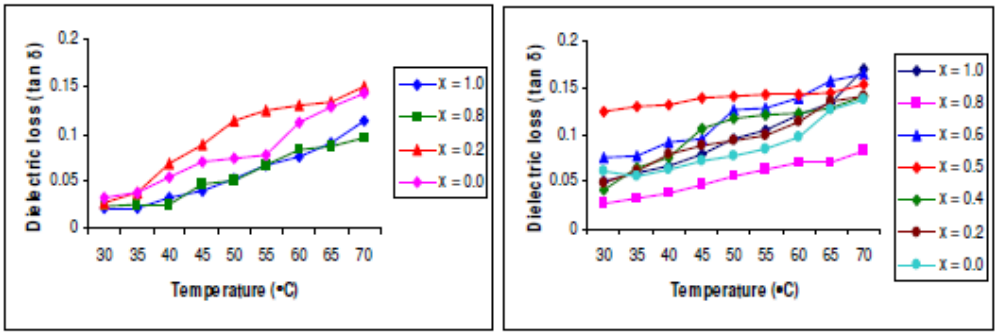

Figure13: Composition dependence of dielectric loss factor for the crystals and crystalline pellets

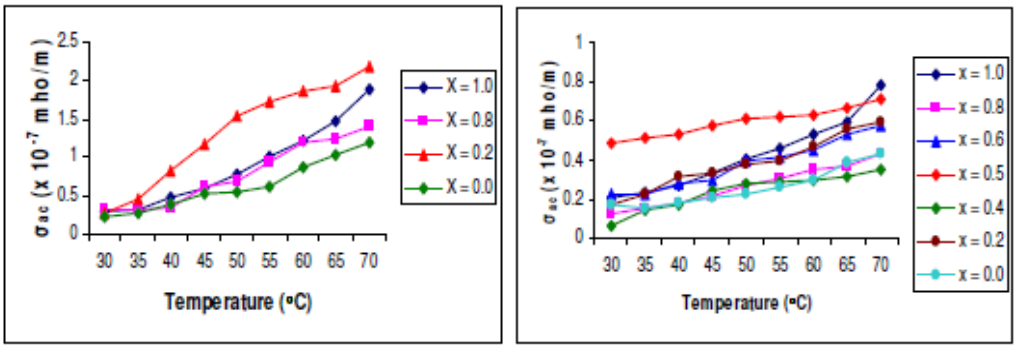

Figure14: Composition dependence of AC electrical conductivity for the crystals and crystalline pellets

ε_r values observed at temperature 30 ° C with 1kHz frequency for the end members (26.14 for BTCC and12.52 for BTCI)are less when compared to those reported earlier[10,2]. (≅125 for BTCC and ≅330 for BTCI). This may be due to the difference in the methods and conditions used for the growth of single crystals. Similarly, the tanδ values observed in the present study are very much less when compared to those reported earlier. This indicates that the crystals grown in the present study are more qualitative and useful in opto-electronic and photonic devices. As in the case of DC conductivity, the ε_r values observed for the crystals studied vary systematically with composition indicating that the ε_r value for BTCI is less than for BTCC. The tanδ and σ_{ac} values for the crystals and ε_r, tanδ andσ_{ac} values for the crystalline pellets vary nonlinearly with the composition. The nonlinear variation of dielectric parameters with composition can be explained as done in the case of DC conductivity.

The material having low dielectric constant will have less number of dipoles per unit volume. As a result, it will have minimum losses as compared to the material having high dielectric constant [8]. The low dielectric losses observed in the present study

indicate that the grown crystals can be expected to be useful for high speed electro-optic devices.

Electrical conductivity of BTCC, BTCI and BTCC-BTCI mixed crystals may be determined by the proton transport within the framework of hydrogen bonds. The proton transport may be accounted for by motion of protons accompanied by a D defect (excess of positive charge). Migration of these defects may only modify electric polarization and may not change the charge at an electrode. The motion of defects occurs by some kinds of rotation in the bond with defects. The speed of displacement $v = \upsilon_a$ where a and υ are the distance and frequency respectively of the jump from one bond to the other [33]. The increase of both DC and AC electrical conductivities with the increase in temperature observed for the crystals considered in the present study can be understood as due to the temperature dependence of the proton transport. Also, the conductivity increases smoothly through the temperature range considered in the present study.

Plots between ln σ_{dc} and $10^3/T$ (not shown here) are found to be nearly linear. So, the conductivity (both DC and AC) values were fitted to the Arrhenius relation as:

$\sigma_{dc}=\sigma_{0dc} \exp[-E_{dc}/ (k T)]$

and $\sigma_{ac}=\sigma_{0ac} \exp[- E_{ac}/ (k T)]$,

where σ_{dc} and σ_{ac} are the proportionality constants (considered to be the characteristic constants of the material), k is the Boltzmann constant and T is the absolute temperature. The activation energies (E_{dc} and E_{ac}) were estimated using the slopes of the corresponding line plots. The estimated E_{dc} and E_{ac} values are found to vary nonlinearly with the composition. Mahadevan and Jayakumari [25] have observed similar nonlinearity in the case of $(NaCl)_x(KCl)_{y-x}(KBr)_{1-y}$ single crystals and attributed it as due to the enhanced diffusion of charge carriers along dislocation and grain boundaries. Results obtained in the present study can also be explained in a similar way.

Table 6: The DC (E_{dc}) and E_{ac} activation energies observed for the crystals and crystalline pellets

$(BTCC)_x(BTCI)_{1-x}$ with	For Crystals		For crystalline pellets	
	E_{dc} (eV)	E_{ac}(eV)	E_{dc} (eV)	E_{ac}(eV)
x = 1.0 (BTCC)	0.499	0.449	0.308	0.311
x = 0.8	0.480	0.385	0.269	0.282
x = 0.6	-	-	0.260	0.227
x = 0.5	-	-	0.119	0.115
x = 0.4	-	-	0.274	0.333
x = 0.2	0.501	0.433	0.172	0.260
x = 0.0 (BTCI)	0.354	0.374	0.321	0.263

The temperature dependence of dielectric constant is generally attributed to the crystal expansion the electronic and ionic polarizations and the presence of impurities and crystal defects. The crystal expansion and ionic polarization are mainly responsible for the variation at lower temperatures. The thermally generated charge carriers and impurity dipoles are mainly responsible for the variation at higher temperatures. In the case of ionic crystals, the electronic polarizability practically remains constant [34]. From the above, it can be understood that the increase in dielectric constant with temperature observed in the present study is essentially due to the temperature variation of ionic polarizability.

4 Conclusions

$(BTCC)_x$ $(BTCI)_{1-x}$ mixed crystals (x = 1.0, 0.8, 0.6, 0.5, 0.4, 0.2 and 0.0) crystals have been successfully formed (grown) by free evoporatoin method and characterized. The crystals grown are found to be stable in atmospheric air, nonhygroscopic and transparent. Mixed crystals with x having the values 0.6, 0.5 and 0.4 are found to be small in size. Results of X-ray

diffraction and FTIR and EDX spectral measurements indicate the possibility of forming mixed crystals based on BTCC and BTCI from the precursors eventhough the crystal lattices of BTCC and BTCI mismatch. The mixed crystals exhibit lower thermal stability and SHG efficiency when compared to the end members. All the seven crystals grown exhibit normal dielectric behavior. The electrical conductivity could be understood as due to the proton transport. The present study, in effect, indicates that mixed crystals can be formed from isomorphous precursors even if the end member crystal lattices mismatch provided the crystals are grown directly from the precursors.

Acknowledgement

One of the authors (I.S.Prameela Kumari) thanks the University Grants Commission (UGC) of India for granting the facility Faculty Development Program (FDP) award

References:

[1] C.K. Lakshman aperumal, A. Arulchakkaravarthi, N.P. Rajesh, P. Santhanaraghavan, Y. C. Huang, M. Ichimura, P. Ramasmamy, *Synthesis, Crystal growth and FTIR, NMR, SHG studies of 4- MethoxyBenzaldihyde-Nmethyl-4-Stilbazolium Tosylate(MBST)*, J. Cryst. Growth. 240(2002) 212-217.

[2] M. Lydia Caroline, S. Vasudevan, *Growth and characterization of bis(thiourea)cadmium iodide: A Semiorganic single crystal*, Mater. Chem. Phys. 113(2009)670-674.

[3] V. Venkataramanan, C.K. Subramanian and H.L. Bhat, *Laser induced damage in zinctris(thiourea) sulfate and bis(thiourea)cadmium chloride*, J. Appl. Phys. 77(1995) 6049-6051.

[4] V. Venkattaramanan, H.L. Bhat, M.R. Sreenivasan, P. Ayub and M.S. Multani, *Vibrational Spectroscopic Study of the Semiorganic Nonlinear Optical Bis(thiourea)cadmium chloride*, J. Raman Specrosc. 28(1997) 779-784.

[5] V. Venkataramanan, S. Maheswaran, J.N. Sherwood, H.L. Bhat , *Crystal growth and physical characterization of the semiorganic bis(thiourea)cadmium chloride*, J.Cryst.Growth 179(1997) 605-610.

[6] P.M. Ushasree, R. Muraleedharan, R. Jayavel, P. Ramasamy, *Growth of bis(thiourea)cadmium chloride single crystals-apotential NLO material of organometallic complex*, J. Cryst. Growth. 218(2000)365-371.

[7] P.M. Ushasree, R. Jayavel, *Growth and micromorphology of as-grown and etched bis(thiourea)cadmium chloride(BTCC) single crystals*, Optical Materials, 21(2002) 599-604.

[8] A. Pricilla Jayakumari, J. Ramajothy, S. Dhanuskodi, *Structural and microhardness studies of a NLO material - bis(thiourea)cadmium chloride*, J.Cryst.Growth 269, (2004) 558-564.

[9] S. Selvakumar, J. Packiam Julius, S.A. Rajasekar, A. Ramanand, P. Sahayaraj, Microhardness, *FTIR and transmission spectral studies of Mg2+ and Zn2+ doped nonlinear optical BTCC* , Mater. Chem. Phys. 89(2005) 244-248.

[10] S. Selvakumar, S.A. Rajaserar, K. Thamizharasan, S. Sreenivasan, A. Ramanand, P. Sagayaraj, *Thermal, dielectric and phoyoconductivity studies on pure,Mg2+ and Zn2+ doped BTCC single crystals*, Mater. Chem. Phys. 93(2005)356-360.

[11] S. Arriponnammal, R. Selva Vennila, S. Radhika, and S. Arumugam, *High pressure electrical resistivity study on nonlinear bis(thiourea)cadmium chloride (BTCC) single crystals Cryst*. Res. Techol. 40, No.9 (2005) 896-897.

[12] S. Ravi, P. Subramanian, *Electron paramagnetic resonance and optical studies of Cu^{2+} doped bis(thiourea)cadmium chloride(BTCC) single crystals* ,Solid State Sciences.(2007) 961-963.

[13] R. Uthrakumar, C. Vesta, C. Justin Raj, S. Dinakaran, Rani Christu Dhas and S. Jerome Das, *Optical and dielectric studies on pure and Ni2+,Co2+,doped single crystals of bis(thiourea)cadmium chloride*, Cryst. Res. Techol. 43,No.4(2008) 428-432.

[14] N.R. Dhunane, S.S. Hussaini, V.G. Dongre, P.P Karmuse, M.D. Shirsat, *Growth and characterization of glysine doped bis(thiourea)cadmium chloride(BTCC) single crystal*, Cryst. Res. Techol. 44, No. 3(2008) 269-274.

[15] J.T. Yang, S.J. Luo, A. Laref, *Mechanism of linear and nonlinear optical properties of bis(thiourea)cadmium chloride single crystals*, Physica B:Condencd Matter, 408(2013) 175-182.

[16] M. Senthilkumar, C. Ramachandraraja, *Studies on the effect of 1 mol% l-alanine*

mixed bis(thiourea)cadmium chloride ,Optik- International Journal for Light and Electron Optics, 124(2013) 1269-1272.

[17] P.A. Angeli Mary, S. Dhanuskodi, *Growth and characterization of a New Nonlinear Optical Crystal: Bis(thiourea) Zinc Chloride*, Cryst. Res. Techol. 36(2001) 1231-1237.

[18] S.K. Kushwaha, N. Vijayan, G. Bhagavanna, *Growth by S R method and characterization of bis(thiourea)zinc(II) chloride single crystals*, Materials Letters 62,No.24,(2008) 3931-3933.

[19] M. Senthilkumar, C. Ramachandraraja, *Growth and Optical Studies on Pure and L-Alanine Mixed Bis(thiourea)cadmium Bromide (LABTCB) Crystals*, Journal of Minerals and MaterialsCharecterization and Engineering,11(2012) 631-639.

[20] G. Pabitha, R. Dhanasekaran, Synthesis, *growth and characterization of tetrathiourea cadmium tetrathiocyanateo zincate single crystals*, J.Cryst.Growth 362(2013)259-263.

[21] M.A. Anie Roshan, Joseph Cyriac and M.A. Ittiyachen, *Cadmium formate NLOsingle crystal*, Mater.Lett. 49(2001) 199-303.

[22] S.K. Kurtz and T.T. Perry, *Apowder technique for the evaluation of nonlinear optical materials* J. Appl. Phys. 39 (1968). 3798-3813.

[23] N. Manonmani, C. K. Mahadevan and V.Umayorubhayan, *Growth and studies of two new potassium compound crystals*, Mater. Manuf.Processes 23(2008)152-158.

[24] M. Meena and C.K. Mahadevan, *Growth and electrical characterization of L-arginine added KDP and ADP single cryastals*, Cryst. Res. Techol. 43(2008), 166-172.

[25] C.K. Mahadevan and K. Jayakumari, *Electrical measurements on multiphased*$(NaCl)_x(KCl)_{y-x}(KBr)_{1-y}$ *Single crystals*, Physica B, 403(2008)3990-3996.

[26] S. Goma, C.M. Padma and C.K. Mahadevan , *Dielectric parameters if KDP single crystals added with urea*, Mater. Lett. 60(2006)3701-3705.

[27] M. Priya and C.K. Mahadevan, *Preparation and dielectric properties of oxide added NsCl-KCl polycrystals*, Physica B: 403(2008) 67-74.

[28] P.M. Ushssre, R. Jayavel, C. Subramanian and P. Ramasay, *Growth, Optical and Electrical Properties of Zinctris(thiourea) sulphate(ZTS) Single Crystals*, J.Cryst.Growth .197(1999),197-216.

[29] Selvasekara Pandian, K. Vivekananandan, P. Kolandaivel and T.K. Gundu Rao, *Vibrational studies of Bis(thiourea)zinc sulphate semiorganic Nonlinear Optical Crystal* ,Cryst. Res. Techol.32(1997)299-309

[30] K.Swaminathan, H.M.N.H.Irving, j.Inorg. Nucl. Chem. 26(1964)1291

[31] U. Lefur, R.Mssse, M.Z.Cherkaoui, J.K.Nicoucl; 2. Kristallogre. 210 (1995)856-

[32] J. Bunget AND m.Popescu, Physics of Solid Dieletrics, Elsevier, New York , 235*1984.

[33] J.M. Kavitha and C. K. Mahadevan, *Growth And Charecterization Of Pure And Glysine Added Morenosite Single Crystals* Int.Journal of Engineering Reaserch and Application, 3 no.5 (2013)1931-1940.

[34] P. Varotsos, *The temperature dependence of the static dieletric constant*, J. Phys. Lett.,39,(1978), L.79-82.